Jefferson Lab PAC16
Proposal Cover Sheet

This document must be received by close of business Thursday, June 8, 1999 at:

Jefferson Lab
User Liaison,
Mail Stop 12B
12000 Jefferson Ave.
Newport News, VA
23606

Experimental Hall: A

Days Requested for Approval: 30

❒ Proposal Title:
Constraining the nucleon strangeness radius in Parity Violating Electron Scattering.

Proposal Physics Goals
Indicate any experiments that have physics goals similar to those in your proposal.

Approved, Conditionally Approved, and/or Deferred Experiment(s) or proposals:

G0 Experiment (Approved)

HAPPEX (Approved)

Contact Person

Name: Krishna KUMAR
Institution: Stanford Linear Accelerator Center
Address: Mail stop 78, SLAC
Address: PO Box 4349
City, State, ZIP/Country: Stanford, CA, 94025
Phone: (650)-926-2794 Fax: 650-926-2923
E-Mail: kkumar@slac.stanford.edu

Jefferson Lab Use Only

Receipt Date: 6/8/99

By: SJC

PR 99-115

BEAM REQUIREMENTS LIST

JLab Proposal No.: ______ Date: ______

Hall: A Anticipated Run Date: ______ PAC Approved Days: ______

Spokesperson: K. Kumar
Phone: (650) 926-2734
E-mail: kkumar@SLAC.Stanford.edu

Hall Liaison: ______

D. Lhuillier (757) 269 69 32
david@jlab.org

List all combinations of anticipated targets and beam conditions required to execute the experiment. (This list will form the primary basis for the Radiation Safety Assesment Document (RSAD) calculations that must be performed for each experiment.)

Condition No.	Beam Energy (MeV)	Mean Beam Current (μA)	Polarization and Other Special Requirements (e.g., time structure)	Target Material (use multiple rows for complex targets — e.g., w/windows)	Material Thickness (mg/cm²)	Est. Beam-On Time for Cond. No. (hours)
1	3200	100	75% Polarization 30Hz helicity reversal	Hydrogen	1062	700 h
2	3200	0.1	"	"	"	16 h

The beam energies, E_{Beam}, available are: $E_{Beam} = N \times E_{Linac}$ where N = 1, 2, 3, 4, or 5. E_{Linac} = 800 MeV, i.e., available E_{Beam} are 800, 1600, 2400, 3200, and 4000 MeV. Other energies should be arranged with the Hall Leader before listing.

LAB RESOURCES LIST

JLab Proposal No.: ____________________ Date ____________________
(For JLab ULO use only.)

List below significant resources — both equipment and human — that you are requesting from Jefferson Lab in support of mounting and executing the proposed experiment. Do not include items that will be routinely supplied to all running experiments such as the base equipment for the hall and technical support for routine operation, installation, and maintenance.

Major Installations *(either your equip. or new equip. requested from JLab)*

Happex detectors needs to be installed in the focal plane of each spectrometer

New Support Structures: ____________________

Data Acquisition/Reduction

Computing Resources: ____________________

New Software: ____________________

Major Equipment

Magnets: Septum magnets that should have been installed for already approved experiments.

Power Supplies: ____________________

Targets: ____________________

Detectors: ____________________

Electronics: ____________________

Computer Hardware: ____________________

Other: ____________________

Other: ____________________

HAZARD IDENTIFICATION CHECKLIST

JLab Proposal No.: ______________________ Date: ______________
(For CEBAF User Liaison Office use only.)

Check all items for which there is an anticipated need.

Cryogenics
- ____ beamline magnets
- ✓ analysis magnets (septum)
- ✓ target

type: 15 K Helium
flow rate: 18 g/s
capacity: 800 W

Electrical Equipment
- ____ cryo/electrical devices
- ____ capacitor banks
- ____ high voltage
- ____ exposed equipment

Radioactive/Hazardous Materials
List any radioactive or hazadorous/ toxic materials planned for use:
____
____
____
____

Pressure Vessels
- ____ inside diameter
- ____ operating pressure
- ____ window material
- ____ window thickness

Flammable Gas or Liquids
type: LH2
flow rate: 0.5 m/s
capacity: 6ℓ (liquid)

Drift Chambers
type: Ethane
flow rate: ~4 ℓ/min
capacity: ____________

Other Target Materials
- ____ Beryllium (Be)
- ____ Lithium (Li)
- ____ Mercury (Hg)
- ____ Lead (Pb)
- ____ Tungsten (W)
- ____ Uranium (U)
- ____ Other (list below)

____
____

Vacuum Vessels
- ____ inside diameter
- ____ operating pressure
- ____ window material
- ____ window thickness

Radioactive Sources
- ____ permanent installation
- ____ temporary use

type: ____________
strength: ____________

Large Mech. Structure/System
- ____ lifting devices
- ____ motion controllers
- ____ scaffolding or
- ____ elevated platforms

Lasers
type: ____________
wattage: ____________
class: ____________

Installation:
- ____ permanent
- ____ temporary

Use:
- ____ calibration
- ____ alignment

Hazardous Materials
- ____ cyanide plating materials
- ____ scintillation oil (from)
- ____ PCBs
- ____ methane
- ____ TMAE
- ____ TEA
- ____ photographic developers
- ____ other (list below)

____
____

General:

Experiment Class:
- ✓ Base Equipment
- ____ Temp. Mod. to Base Equip.
- ____ Permanent Mod. to Base Equipment
- ____ Major New Apparatus

Other: ____________
____

HALL A

HAPPEX II EXPERIMENT

COMPUTING REQUIREMENTS:

Amount of raw data expected: ~75 GB

Computing power required for analysis:
Equivalent to some hours CPU time on jlabs1.

Amount of on-line disk storage:
~100 GB for all the raw data + hbook files + codes.

All data will need to be copied on DLTs
for the Saclay collaboration.

Proposal to Jefferson Lab PAC 16

CONSTRAINING THE NUCLEON STRANGENESS RADIUS IN PARITY VIOLATING ELECTRON SCATTERING

R. De Leo, L. Lagamba
INFN/Bari

D.J. Margaziotis
California State University

P. Markowitz
Florida International University

R. Wilson
Harvard University

A.T. Katramatou, G.G. Petratos, D.L. Prout
Kent State University

R. Hicks, R. Miskimen, G. Peterson
University of Massachusetts

J. Calarco, W. Hersman, M. Leuschner
University of New Hampshire

G.D. Cates, B. Humensky, K.S. Kumar (Co-spokesperson), D. Relyea
Princeton University

M. Amarian, E. Cisbani, S. Fullani, F. Garibaldi, M. Iodice, R. Iommi, G.M. Urciuoli
INFN/Rome

E. Burtin, C. Cavata, B. Frois, D. Lhuillier (Co-spokesperson),
F. Marie, D. Neyret, T. Pussieux
DSM/DAPNIA/SPhN CEA Saclay

P.A. Souder, R. Holmes
Syracuse University

L. Auerbach, S. Choi and Z. Meziani
Temple University

J.P. Chen, E. Chudakov, K. De Jager, J. Gomez, M. Kuss, J. LeRose,
M. Liang, R. Michaels, J. Mitchell, A. Saha, B. Wojtsekhowski
Thomas Jefferson National Accelerator Facility

D. Armstrong, T. Averett, J.M. Finn, J. Roche
College of William and Mary in Virginia

(This is a Hall A Collaboration Proposal)

ABSTRACT

We propose to measure the parity violating asymmetry in the elastic scattering of 3.2 GeV electrons from a liquid Hydrogen target in Hall A at a scattering angle of $\theta_{\mathrm{lab}} = 6°$, corresponding to an average Q^2 of 0.11 $(\mathrm{GeV/c})^2$. The small scattering angle will be achieved with a combination of the HRS high resolution spectrometers and septum magnets that are planned to be installed in Hall A. The physics asymmetry is estimated to be about 1.7 parts per million. With 100μA electron beam and a polarization of 75%, a statistical error of 4.6% and a projected systematic error of 2.9% can be achieved in 700 hours. The recent physics run of the HAPPEX experiment has demonstrated that systematic errors can be controlled at the required level with a high polarization photocathode.

This measurement would access the linear combination $\rho_s + \mu_p \mu_s$ to an accuracy of ± 0.31 and would provide a direct sensitive constraint on the nucleon strangeness radius. The experiment would thus probe the importance of strangeness to the charge distribution inside nucleons and could potentially make a clean, nonzero measurement of a nucleon strangeness matrix element.

I INTRODUCTION

Several lepton and hadron scattering experiments have recently focused on the issue of the strange structure of the nucleon. Establishing a nontrivial role for the nucleon sea would provide spectacular evidence for new nonperturbative strong dynamics. While there are intriguing suggestions for nonzero strange matrix elements, there is no consensus in the theoretical interpretation of the results.

Measurements of parity violating asymmetries in elastic electron scattering are a natural way to access vector strange matrix elements [1,2]. Recently, the SAMPLE [3] and the HAPPEX [4] experiments have carried out measurements of such asymmetries off protons at $Q^2 \sim 0.1$ (backward angle) and 0.5 $(\mathrm{GeV/c})^2$ (forward angle) respectively. In parallel, theoretical models have tackled quantitatively the leading nonzero moments of the strange quark form factors: the strange magnetic moment μ_s and the strangeness radius ρ_s [5]. The results of the abovementioned pioneering experiments have ruled out a large value of μ_s and suggest that if ρ_s is large then the strange form factors must fall rapidly with Q^2. However, there is as yet little theoretical guidance on the Q^2 dependence of the strange form factors.

We propose a new measurement that focuses on the leading moments with little sensitivity to the Q^2 dependence of the form factors. In this proposal, we would measure the parity violating asymmetry in the elastic scattering of 3.2 GeV electrons from protons at $\theta_{\mathrm{lab}} = 6°$ ($Q^2 = 0.11$ $(\mathrm{GeV/c})^2$) in Hall A. A relative accuracy of $\pm 4.6\%$(stat) $\pm 2.5\%$(syst) $\pm 1.4\%$(theo) can be achieved in 700 hours at a beam current of 100 μA and a beam polarization of 75%. From this measurement, we would obtain the linear combination $\rho_s + \mu_p \mu_s$ with an accuracy of ± 0.31. When combined with the anticipated uncertainty of the SAMPLE experiment, the Dirac strangeness radius $\langle r_s^2 \rangle$ would be constrained to $\pm 0.04 fm^2$.

The experiment is a natural sequel to the HAPPEX measurement, which established the feasibility of high accuracy, high luminosity parity violation experiments in Hall A at Jefferson Lab. The most recent run of the HAPPEX experiment has further demonstrated that the potentially larger systematic problems associated with the high polarization strained photocathode can be controlled at the required level.

II PHYSICS MOTIVATION

The Valence Quark Model has provided valuable insights into the structure of baryons. On the other hand, the dynamical origin of the nucleon sea remains elusive. Indeed, one of the central issues in nucleon strong dynamics today is the justification of the success of the Quark Model: why is the $q\bar{q}$ sea, which originates from nonperturbative effects, so highly inert? It is thus interesting to probe asymmetries and moments of sea quark distributions experimentally. Indeed, different theoretical approaches produce widely differing predictions for various sea quark distributions.

Strange quarks are a direct, pure probe of the nucleon sea and thus a particularly fertile testing ground for various QCD models. Since $m_s \sim \Lambda_{\rm QCD}$, it is quite plausible that strange quarks play a nontrivial role in determining fundamental bulk nucleon properties. On the other hand, the empirically successful OZI rule suggests that strange quark effects are highly suppressed at low energy. The issue must be settled by experiment. However, the goal of making a compelling measurement of a strange matrix element has proved to be challenging.

Experimental measurements to date come from the area of $\pi - N$ and spin dependent deep inelastic lepton scattering experiments. Spin structure function measurements indicate that only ~30-40% of the proton spin is carried by quarks. When this data is combined with measurements of hyperon decay rates, the resulting analysis suggests that ~10% of the proton spin is carried by strange quarks. However, this effect may be explained by flavor SU(3) breaking and is an area of active theoretical and experimental debate. An additional indication comes from the pion σ term from an analysis of low energy $\pi - N$ scattering, which suggests that the strange quark scalar matrix element contributes significantly to the proton mass.

II.1 Parity Violating Electron Scattering

The results described above motivate the search for other strange matrix elements. A clean experimental technique [6] for isolating vector strange matrix elements is by measuring parity-violation amplitudes in the elastic scattering of polarized electrons from nucleons and nuclei [1,2]. One measures an asymmetry defined by

$$A^{PV} = \frac{\sigma_R - \sigma_L}{\sigma_R + \sigma_L} \tag{1}$$

where σ_R (σ_L) is the scattering cross section using incident right (left) handed electrons.

The theoretical asymmetry is given in the Standard Model by [5]

$$A^{PV} = \left[\frac{-G_F Q^2}{\pi\alpha\sqrt{2}}\right] \times \frac{\varepsilon G_E^{p\gamma} G_E^{pZ} + \tau G_M^{p\gamma} G_M^{pZ} - \frac{1}{2}(1 - 4\sin^2\theta_W)\varepsilon' G_M^{p\gamma} G_A^{pZ}}{\varepsilon (G_E^{p\gamma})^2 + \tau (G_M^{p\gamma})^2} \tag{2}$$

where G_F is the Fermi coupling constant and $G_E^{p\gamma}(G_M^{p\gamma})$ is the electric(magnetic) Sachs form factor for photon exchange, $G_{E,M}^{pZ}$ is the corresponding quantity for Z^0 exchange and θ_W is the electroweak mixing angle. All form factors are functions of Q^2 and ε, τ, and ε' are kinematic quantities.

To interpret the experiment, $G^{p,Z}_{E,M}$ can be expressed in terms of proton, neutron, and strange form factors if the up(down) quarks in the proton have the same properties as the down(up) quarks in the neutron (assumption of isospin symmetry). Then

$$G^{p,Z}_{E,M} = \frac{1}{4}(G^{p\gamma}_{E,M} - G^{n\gamma}_{E,M}) - \sin^2\theta_W \, G^{p\gamma}_{E,M} - \frac{1}{4}G^{s}_{E,M} \tag{3}$$

and, if the electromagnetic form factors are sufficiently well known from experiment, the only unknown quantities involve strange form factors.

II.2 Theoretical Predictions

Given the impact of potentially large strange quark effects in the nucleon, significant theoretical effort has been applied to obtaining a quantitative understanding of the strange quark form factors. This is challenging and effort has been focused on the leading nonzero moments of the strange quark form factors:

$$\mu_s \equiv G^s_M(0); \quad \rho_s \equiv \left.\frac{dG^s_E}{d\tau}\right|_{\tau=0}. \tag{4}$$

It is often more convenient to talk about a strangeness Dirac rms radius, in analogy to the charge radius, which is related to the above quantities as follows:

$$\langle r^2_s \rangle \equiv -6\frac{dF^{s2}_1}{dQ^2}; \quad \rho_s = -\frac{2}{3}M^2_p\langle r^2_s\rangle - \mu_s. \tag{5}$$

Here, F^s_1 is the Dirac strange form factor and M_p is the nucleon mass.

Lattice QCD, hadronic models and effective hadronic theory are three broad approaches that have been used to estimate the abovementioned quantities [7]. Theoretical predictions vary widely and are not consistent in the predicted sign for ρ_s. Further, at this stage there is little insight into the Q^2 dependence of the form factors. We present a brief discussion on some aspects of the literature below as an introduction. Some of the results on the leading moments are tabulated in Table 1.

One approach is to use dispersion theory fits to the nucleon isoscalar form factors [9], updated to account for new data and constraints from peturbative QCD at large Q^2 [10]. Such an approach predicts a sizeable strange radius. On the other hand, it has been pointed out that the inclusion of $\pi\rho$ correlated exchange is significant and might reduce the predicted size of the strange vector form factors [11]. The authors of Ref. [12] added the $K\bar{K}$ continuum contribution in addition to the usual vector meson poles. They found that the magnitude and sign of μ_s is rather robust but find that predictions for ρ_s vary over a wide range.

Source	$r_s(fm^2)$	ρ_s	μ_s	$\rho_s + \mu_p\mu_s$	Reference
Poles	0.16	-2.10	-0.31	-2.97	[9]
Poles (update)	0.21	-2.93	-0.24	-3.60	[10]
Poles + $K\bar{K}$	-0.15 - +0.42	-6.0 - +2.65	-0.51 - -0.26	-7.10 - -1.23	[12]
NJL model	-0.2	3.06	-0.05	2.92	[13]
SU(3) Skyrme	-0.19	3.19	-0.33	2.27	[14]
SU(3) Skyrme broken sym.	-0.10	1.64	-0.13	1.27	[15]
Lattice	-0.16 - -0.06	1.26 - 2.77	-0.56 - -0.16	0.25 - 1.76	[16]
Quark Model	-0.04	0.57	0.035	0.67	[17]

TABLE 1. Various predictions of the strangeness radius and magnetic moment.

In addition to the dispersion approach, there exists a quark model calculation in which a sum over a tower of OZI-allowed states is performed [17]. The authors find that both the leading moments are small. Recently, lattice QCD techniques have also begun to yield predictions for the leading moments of the strange form factors [16].

In summary, predictions for μ_s are either very small or fall within the range -0.2 to -0.4 μ_N. Predictions for ρ_s on the other hand vary over a large range and are typically considered more speculative in most approaches. The HAPPEX experiment that is currently running in Hall A is the first experiment to have significant sensitivity to the strange electric form factor. The projected sensitivity from the '99 run on ρ_s depends on the assumed Q^2 dependence of the strange form factors, but a conservative estimate is that the sensitivity of the measurement is roughly the size of the neutron charge radius. Our measurement would provide a constraint that is three times smaller than the size of the neutron charge radius. Such sensitivity would access the range of values favored by theoretical predictions and would address whether strangeness is an important degree of freedom in the charge distribution inside nucleons.

II.3 Experimental Strategy

From Table 1, it is clear that a measurement of $\langle r_s^2 \rangle$ to better than ± 0.05 would be an important step in addressing the issue of strangeness in nucleons. In order to achieve this level of accuracy, we wish to go to sufficiently low $Q^2(\sim 0.1\ (\mathrm{GeV/c})^2)$ so that information on the leading moments ρ_s and μ_s can be obtained with little dependence on the Q^2 behavior of the form factors.

Our first priority in optimizing the experimental design is to obtain a sensitive measurement of ρ_s, on which no clean experimental constraints are available to date. The best available constraint can be derived from the HAPPEX measurement at $Q^2 = 0.48\ (\mathrm{GeV/c})^2$, though additional assumptions on the Q^2 dependence for the strange electric as well as magnetic form factors are required. The projected errors (when the '99 data is analysed) range from ± 0.05

to $\pm 0.12 fm^2$, depending on assumptions. The two logical target choices for new measurements at low Q^2 are ^{1}H and ^{4}He.

Hydrogen has the advantage that one is directly probing the nucleon and one can employ a dense target. Further, the fractional error on the asymmetry that leads to useful constraints on strangeness tends to be at the 10% level. One disadvantage is that one is measuring the linear combination $\rho_s + \mu_p \mu_s$. Additionally, as Q^2 is lowered, the nuclear structure independent piece of the asymmetry ($1 - 4\sin^2\theta_W$ term in Eq. 6) begins to dominate the weak neutral coupling so that it becomes increasingly difficult to obtain precise information on the form factors.

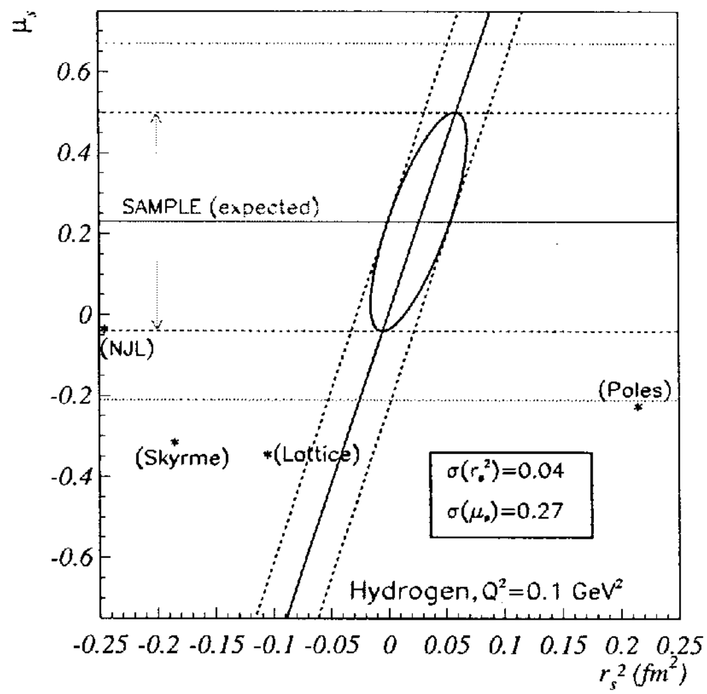

FIGURE 1. The sensitivity of the proposed ^{1}H measurement is shown. Also shown are the published and projected errors from the SAMPLE experiment, centered at the published value. Stars correspond to various theoretical predictions listed in Table 1.

Helium has the advantage that one is directly measuring ρ_s. Moreover, the theoretical ambiguities in considering the nucleus as a spinless, isoscalar coherent state of four nucleons are estimated to be small. The disadvantages are that it is difficult to get a target as dense as that for hydrogen and further, one needs to measure the asymmetry at the 5% level in order to obtain useful constraints on strangeness.

We have investigated the feasibility of both measurements and find that they lead to similar constraints on the strange radius for the same beam current. This proposal focuses on ^{1}H for two technical reasons. Firstly, the target system for hydrogen already exists and has been demonstrated to work at the highest luminosities that we propose to use for this experiment. Secondly, the absolute normalization for ^{1}H is less stringent than that required for the ^{4}He measurement. Figure 1 shows the achievable errors on $\langle r_s^2 \rangle - \mu_s$ from the ^{1}H measurement. Also shown are the current and anticipated error bars of the SAMPLE experiment.

III CHOICE OF KINEMATICS

The choice of our running conditions is driven by our sensitivity to the linear combination $(\rho_s + \mu_p \mu_s)$. Using the definition of Eq.(4) and expanding the expression of the parity violating asymmetry (2) to first order in Q^2 yields

$$A^{PV} = -\frac{G_F Q_2}{4\pi\alpha\sqrt{2}} \left[(1 - 4\sin^2\theta_W) + \tau(\mu_n - \rho_s - \mu_p(\mu_n + \mu_s))\right] + \mathcal{O}(\tau^2) \quad (6)$$

where we have used the small angle approximations $\epsilon' \simeq 0$, $\epsilon \simeq 1$, and $\tau \ll 1$. The absolute statistical error on $\rho_s + \mu_p \mu_s$ is then

$$\delta(\rho_s + \mu_p \mu_s) = \left(\frac{1 - 4\sin^2\theta_W}{\tau} + \mu_n(1 - \mu_p)\right) \times \frac{\delta A^{PV}}{A^{PV}} + \mathcal{O}(\tau^2) \quad (7)$$

Figure (2) shows the corresponding figure of merit (FOM) as a function of the two free parameters of the elastic kinematics, the scattering angle and the beam energy. We can see that at very low Q^2 (small θ and low E_{beam}), the

E_{beam} (GeV)	θ (deg)	Q^2 (GeV^2)	$d\Omega$ (msr)	$\delta A^{PV}/A^{PV}$ (%)	$\delta(\rho_s + \mu_p \mu_s)$
3.2	6.00	0.110	2×3.60	4.3	0.25
2.4	7.64	0.100	2×3.60	5.9	0.35
1.6	12.50	0.117	2×5.50	6.7	0.38

TABLE 2. Projected statistical error bars after 700h beam time for three kinematics at $Q^2 \simeq 0.1\,GeV^2$. Detection below 12.5° requires a septum magnet which reduces the acceptance of the spectrometer. A cut in the radiative tail is applied at 1% of the elastic energy. Results are obtained from average values in the plane of the collimator.

sensitivity to strangeness in the nucleon falls off. Simulations including finite acceptance and extended target effects, as well as radiative corrections show that the best compromise is to relax the constraint on the beam energy and stay at small scattering angle to take advantage of the high counting rates.

Assuming a 100μA beam current, 75% beam polarization and the target properties given in Table 5 we then obtain a luminosity of $\mathcal{L} = 3.96 \times$

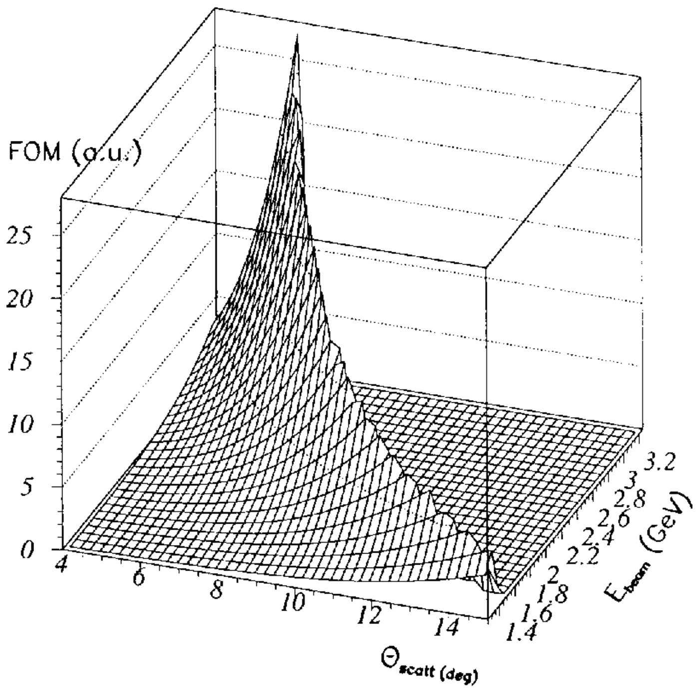

FIGURE 2. Figure Of Merit for the measurement of strange form factors in elastic e-P scattering. Only the kinematical domain $Q^2 < 0.25\,GeV^2$ is represented. The plotted quantity is the square of $\delta(\rho_s + \mu_p\mu_s)^{-1}$ (Eq.7). The solid angle is assumed constant over all the kinematic range, the elastic cross section is calculated using a dipole form factor and the contribution from strange quarks is set to zero in the parity violating asymmetry.

$10^{38}\,cm^{-2}s^{-1}$. Table 2 shows the projected statistical error bars after 700h with these running conditions for three kinematic points at $Q^2 \simeq 0.11$ GeV^2. The current minimum central angle of the Hall A HRS is 12.5°. To go to smaller scattering angles, our experiment will use septum magnets, inserted between the scattering chamber and the entrance of the HRS. This apparatus is being designed by the Hall A Hypernuclear Collaboration [18] and will be mounted next year. It will allow the detection of scattered electrons as forward as 6°. The HRS pair can detect electrons with a maximum momentum of 3.1 GeV. We therefore choose to run the experiment at this minimum angle and a beam energy of 3.2 GeV.

Rates and kinematics corresponding to $E_{beam} = 3.2$ GeV and $\theta = 6°$ are listed in Table 3. Central and average values are comparable because of the cancellation of two main effects. The finite acceptance opens the phase space to larger scattering angles, which decreases the cross section. On the other hand, emission of real photons by the electrons lowers the effective Q^2 and thus increases the mean cross section. Figure 3 plots the expected statistical error bars for the asymmetry and the accessed linear combination of the strange

	θ (deg)	Q^2 (GeV^2)	$d\Omega$ (msr)	$d\sigma/d\Omega$ $(\mu b.sr^{-1})$	A^{PV} (ppm)	Rate (Mhz)
Central Value	6.00	0.110	2×3.57	44.83	-1.67	127.8
Average Value	5.93	0.109	2×3.57	44.45	-1.63	126.8

TABLE 3. Central values correspond to the kinematics of a scattered electron following the reference trajectory of the spectrometer. Average values take into account the effects of finite acceptance, extended target, radiative losses and tracking through the spectrometers. The cut in the radiative tail is taken to be 1% of the energy of the elastic peak ($\Delta E \simeq 30 MeV$, 10% losses). The quoted counting rates include the sum over the two Hall A spectrometers. Values of A^{PV} are for 100% beam polarization.

form factors as a function of the beam time:

$$\frac{\delta A^{PV}}{A^{PV}} = \frac{1}{P_e A^{PV}} \times \frac{1}{\sqrt{\mathcal{L}\frac{d\sigma}{d\Omega}d\Omega}} \times \frac{1}{\sqrt{T}}$$

$$\delta(\rho_s + \mu_p\mu_s) = \left[\frac{1 - 4\sin^2\theta_W}{\tau} + \mu_n(1 - \mu_p)\right] \times \left[\frac{\delta A^{PV}}{A^{PV}}\right]$$

A statistical accuracy of 4.6% is achievable in the asymmetry in 700 hours. The corresponding uncertainty in the linear combination of ρ_s and μ_s is $\delta(\rho_s + \mu_p\mu_s) = \pm 0.25$.

IV APPARATUS

The experimental design is driven by the fact that one is measuring a small parity violating asymmetry of the order of 1 part per million (ppm). To measure such an asymmetry with little contamination from spurious effects, one needs to rapidly flip (in time) between the two possible electron helicity states while keeping all other experimental parameters virtually unchanged. One then averages the fractional difference in the cross-section over many pairs of beam "windows" of opposite helicity.

Our measurement technique will follow the methods employed for the published HAPPEX measurement which takes advantage of the high resolution spectrometers in Hall A. We note the key features:

- We integrate the scattered flux over each helicity window. The current set up has already been demonstrated to work at 50 MHz and can be realistically extrapolated to 200 MHz.
- The scattered flux from each spectrometer is digitized using custom built ADCs.

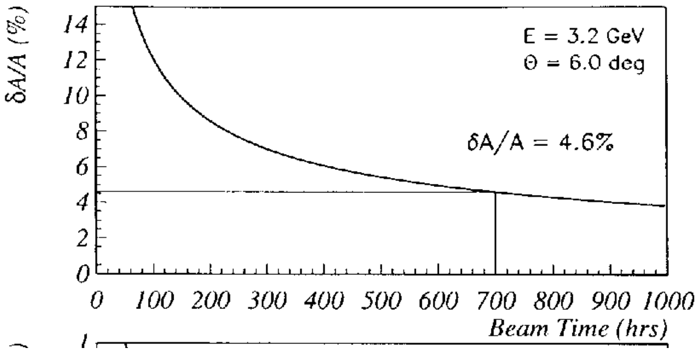
E = 3.2 GeV
Θ = 6.0 deg
δA/A = 4.6%
δA/A (%)
Beam Time (hrs)